Dicoumarol attenuates NLRP3 inflammasome activation to inhibit inflammation and fibrosis in knee osteoarthritis

WENJIE GE[1,2], XIAN ZHANG[1], QING WANG[1], JIANJIE MAO[1], PENGFEI JIA[1] and JIANPING CAI[1]

[1]Department of Orthopedics and Traumatology, Wuxi Hospital of Traditional Chinese Medicine Affiliated to Nanjing University of Chinese Medicine; [2]Department of Orthopedics and Traumatology, Jiangsu CM Clinical Innovation Center of Degenerative Bone and Joint Disease, Wuxi Hospital of Traditional Chinese Medicine Affiliated to Nanjing University of Chinese Medicine, Wuxi, Jiangsu 214000, P.R. China

Received March 15, 2023; Accepted February 23, 2024

DOI: 10.3892/mmr.2024.13224

Abstract. Knee osteoarthritis (KOA) is a major cause of disability in elderly individuals. Dicoumarol is a coumarin-like compound derived from sweet clover [*Melilotus officinalis* (L.) Pall]. It has been suggested that dicoumarol exhibits various types of pharmacological activities, including anticoagulant, antitumor and antibacterial effects. Due to its various biological activities, dicoumarol has a potential protective effect against OA. Therefore, the present study aimed to assess the effects of dicoumarol on knee osteoarthritis. In the present study, dicoumarol was found to protect rat synoviocytes from lipopolysaccharide (LPS)-induced cell apoptosis. Western blot analysis showed that dicoumarol significantly reduced the protein expression levels of fibrosis-related markers and inflammatory cytokines (*Tgfb*, *Timp*, *Col1a*, *Il1b* and *Il18*). The inhibitory rates of these proteins were all >50% (P<0.01) compared with those in the LPS and ATP-induced group. Consistently, the mRNA expression levels of these markers and cytokines were decreased to normal levels by dicoumarol after the treatment of rat synovial fibroblasts with LPS and ATP. Mechanistic studies demonstrated that dicoumarol did not affect NF-κB signaling, but it did directly interact with NOD-like receptor protein 3 (NLRP3) to promote its protein degradation, which could be reversed by MG132, but not NH_4Cl. The protein half-life of NLRP3 was accelerated from 26.1 to 4.3 h by dicoumarol. Subsequently, dicoumarol could alleviate KOA *in vivo*; knee joint diameter was decreased from 11.03 to 9.93 mm. Furthermore, the inflammation and fibrosis of the knee joints were inhibited in rats. In conclusion, the present findings demonstrated that dicoumarol could impede the progression of KOA by inhibiting NLRP3 activation, providing a potential treatment strategy for KOA.

Correspondence to: Professor Jianping Cai, Department of Orthopedics and Traumatology, Wuxi Hospital of Traditional Chinese Medicine Affiliated to Nanjing University of Chinese Medicine, 8 Zhongnan West Road, Wuxi, Jiangsu 214000, P.R. China
E-mail: 2054871367@qq.com

Key words: knee osteoarthritis, dicoumarol, NOD-like receptor protein 3, inflammation, fibrosis

Introduction

Knee osteoarthritis (KOA) is a chronic disease (1-3), during which patients suffer from persistent painful arthritis. KOA is characterized by progressive destruction of articular cartilage, synovial inflammation, fibrosis, osteophyte formation and subchondral bone changes, which can lead to pain, stiffness and chronic disability (4-6). Approximately 250 million people are currently affected by KOA worldwide, and there is no effective drug for KOA treatment (7,8).

It has been reported that inflammation serves a key role in the pathogenesis of KOA (1,9-12). The activation of the NOD-like receptor protein 3 (NLRP3) inflammasome initiates the inflammatory cascade, and it is closely related to a number of types of chronic inflammation (13). Thus, inhibition of NLRP3 inflammasome activation has been demonstrated to ameliorate a variety of fibrotic diseases, including synovial fibrosis in KOA (14). The NLRP3 inflammasome consists of a sensor (NLRP3), an adaptor [apoptosis-related speckle-like protein (ASC)/PYCARD] and an effector (caspase-1) (15-17). When cells are stimulated, ASC interacts with the caspase recruitment domain to assemble into a macromolecular complex, which assembles the NLRP3 inflammasome (18,19). Subsequently, the complex cleaves caspase-1, leading to maturation of caspase-1. Subsequently, active caspase-1 cleaves gasdermin-D (GSDMD) and induces the secretion of interleukin (IL)-1β and IL-18, which results in cartilage degeneration and synovial membrane inflammation (20,21). Recent research has revealed that inhibiting NLRP3 activation reduces synovial inflammation and fibrosis in KOA (22-24).

Coumarins comprise a large class of natural phenolic compounds found in traditional medicinal herbs, such as Rutaceae, Umbelliferae, Compositae and Leguminosae, which have been reported to show antioxidant and anti-inflammatory activity (25,26). As one of the derivatives in coumarins, dicoumarol was first discovered from the spoilage of *Melilotus officinalis* (L.) Pall. Due to its molecular structural similarity to vitamin K, dicoumarol has been used as an anticoagulant and can reversibly compete with vitamin K to

prevent the formation of thrombi (25,27,28). However, there are no studies reporting the relationship between dicoumarol and inflammation. Therefore, the present study aimed to explore whether dicoumarol has a potential protective effect against KOA based on its various biological activities.

Materials and methods

Compounds. Dicoumarol was purchased from Shanghai Aladdin Biochemical Technology Co., Ltd. Dicoumarol was dissolved in dimethyl sulfoxide (DMSO) as a stock solution, stored at -20˚C, and freshly diluted with medium to the final concentration used *in vitro* studies. The final concentration of DMSO was <0.1%.

Rat KOA model and experimental design. A total of 26 3-month-old Sprague-Dawley (SD) male rats weighing from 280 to 320 g (Beijing Vital River Laboratory Animal Technology Co., Ltd.) were housed in a specific pathogen-free (SPF)-grade environment at 25±2˚C with a relative humidity of 50-60%, and provided with food and water *ad libitum*. Rats were divided into the following three groups: Normal (vehicle) group (n=7), KOA group (n=7) and KOA + dicoumarol group (n=7). All animal experiments were performed according to the National Institute of Health Animal Care and Use Guidelines (29), and the protocol was approved by the committee for the Ethics of Animal Experiments, Wuxi Hospital of Traditional Chinese Medicine (Wuxi, China; approval no. SWJWQNXM2020033102). Before the operation, the SD rats were fasted and deprived of water for 12 h. Animals were anesthetized with 2% isoflurane mixed with oxygen via inhalation and were maintained on the same concentration of anesthetic throughout the entirety of the procedure. Briefly, a syringe was used to inject a suspension of monosodium iodoacetate (MIA; 5 mg/ml; MilliporeSigma) into the knee joint cavity (30). Postoperatively, the rats were closely monitored to ensure their comfort and wellbeing, with prompt identification of any signs of discomfort or complications. Drug administration commenced on day 7 post-modeling, and knee joint diameter was measured every 7 days thereafter. The normal group and the KOA group were administered normal saline via intragastric administration as the control, and each rat in the KOA + dicoumarol group was treated with 10 mg/kg dicoumarol every day via intragastric administration. Doses were chosen with reference to previous studies (31). In addition, several pre-experiments were performed to select the dose of dicoumarol, with the selection criteria being both significant relief of KOA in rats and achieving good compliance in rats (data not shown). On day 28, the rats were anesthetized with 2% isoflurane mixed with oxygen via inhalation and were maintained on the same concentration of anesthetic throughout the entirety of the procedure the rats were euthanized and separate knee joint tissues for further experiments. Animals were sacrificed by intraperitoneal administration of an overdose of 1-1.5 ml pentobarbitone (150-200 mg/kg), which amounted to 64.8 mg/ml pentobarbitone. Death was confirmed by checking for cardiac arrest, after which the animal was observed for ~5 min.

Cell preparation and treatment. For FLS isolation, knee joint tissues removed from healthy SD rats (weight, 280-320 g; age, 3 months; Beijing Vital River Laboratory Animal Technology Co., Ltd.) were snipped into 1-3 mm^3 pieces, homogenized in DMEM (Gibco; Thermo Fisher Scientific, Inc.) and incubated for 1 h at 37˚C with 1 mg/ml type I collagenase (MilliporeSigma). The samples were then filtered through a 100-μm cell strainer. After dissociation, the FLSs were pelleted via centrifugation at 300 x g at ~25˚C for 5 min and plated in DMEM supplemented with 10% FBS (Gibco; Thermo Fisher Scientific, Inc.) and 1% antibiotics (penicillin and streptomycin; Gibco; Thermo Fisher Scientific, Inc.). Cells were cultured at 37˚C in a humidified atmosphere with 95% air and 5% CO_2. Primary FLSs from passages 3-5 were used for subsequent experiments. All animal experiments were performed according to the National Institute of Health Animal Care and Use Guidelines (29), and the protocol was approved by the Committee for the Ethics of Animal Experiments, Wuxi Hospital of Traditional Chinese Medicine (Wuxi, China; approval no. SWJWQNXM2020033102).

FLSs were initially stimulated with lipopolysaccharide (LPS; 10 ng/ml) for 12 h at 37˚C, followed by a 3-h incubation with ATP (5 mM) at 37˚C, to simulate the inflammatory environment of KOA and to activate the NLRP3 inflammasome. Subsequently, the FLSs were treated with dicoumarol (30 μM) for an additional 12 h before proceeding with subsequent experiments. The doses of LPS and ATP were chosen with reference to previous studies (14,32). LPS and ATP were obtained from MilliporeSigma.

Degradation assay. Cycloheximide (CHX), MG132 and NH_4Cl were obtained from MilliporeSigma, and concentrations were chosen as described previously (33). Compounds used in assays were dissolved in DMSO and kept as 10 mM stock solutions for *in vitro* studies (33). The final concentration of DMSO was <0.1%.

Briefly, FLSs were pretreated with dicoumarol (30 μM) or DMSO for 12 h, followed by the addition of CHX (10 μM) for 0, 2, 4, 8, 12 and 24 h at 37˚C, after which the cells were harvested. In addition, FLSs were stimulated with LPS (10 ng/ml) for 12 h, followed by a 3-h stimulation with ATP (5 mM). After a 12 h treatment with dicoumarol (30 μM), the cells were then treated with NH_4Cl (10 μM) or MG132 (10 μM) for 8 h and the cells were collected.

Cellular thermal shift assay (CETSA). First step: FLSs were initially treated with DMSO or dicoumarol. For each group, $3x10^7$ cells were harvested after 1 h of culturing with DMSO or dicoumarol (50 μM). Subsequently, the cells were transferred to EP tubes and were heat shocked for 3 min each at 43.5, 44.5, 45.9, 48, 50, 52.7, 55, 57.2, 59.5, 61.5, 62.7 and 63.5˚C. The samples were then subjected to three freeze-thaw cycles. For each cycle, cells were exposed to liquid nitrogen for 1 min and placed in a heating block at 25˚C. The sample-containing tubes were then centrifuged at 15,000 x g for 15 min at 4˚C to precipitate the cell debris. The soluble supernatant was used for western blotting. Second step: Next, for determination of the isothermal concentration-response fingerprint for NLRP3, cells were incubated with DMSO or different concentrations of dicoumarol for 30 min at 37˚C. Cells were then heated at

57.2˚C, as calculated in the first step, for 3 min and placed in an aluminum block at room temperature for 3 min. Western blotting was then performed on the supernatant.

Sirius Red staining. Synovial tissues sections from rats in the Control, KOA and KOA + dicoumarol groups underwent staining. The frozen knee joint tissues sections (5 μm) were removed from the -20˚C freezer and restored to room temperature, they were then fixed with 4% paraformaldehyde for 15 min at room temperature and rinsed with running water. The sections were stained with 100% Sirius Red staining solution (Wuhan Servicebio Technology Co., Ltd.) for 8 min at room temperature. The sections were sequentially soaked in 70, 90 and 100% ethanol for 10 sec at room temperature for dehydration, followed by 5 min in xylene. Finally, neutral resin was applied to the center of the sections and a coverslip was added. Tissue changes were observed under a light microscope (ZEISS Axio Vert. A1; Carl Zeiss AG).

Hematoxylin and eosin (H&E) staining. Synovial tissues sections from rats in the Control, KOA and KOA + dicoumarol groups underwent staining. The frozen knee joint tissues sections (5 μm) were removed from the -20˚C freezer and restored to room temperature, they were then fixed with 4% paraformaldehyde for 15 min at room temperature and rinsed with running water. The sections were stained with 100% hematoxylin (Wuhan Servicebio Technology Co., Ltd.) for 5 min at room temperature. Subsequently, the sections. The sections were sequentially soaked in 85 and 95% ethanol for 5 min at RT for dehydration. Next, the sections were stained with 100% eosin staining solution (Wuhan Servicebio Technology Co., Ltd.) for 5 min at room temperature. Tissue changes were observed under a light microscope (ZEISS Axio Vert. A1).

Immunohistochemistry. Synovial tissues sections from rats in the Control, KOA and KOA + dicoumarol groups underwent immunohistochemistry analysis. The synovial tissues were fixed with 4% formalin for 20 h at room temperature, embedded in paraffin and sections were prepared (7 μm). The consecutive serial sections were deparaffinized with xylene and rehydrated in an alcohol gradient. The sections were immersed in sodium citrate and heated in a microwave at 800 W for 3 min and then left for 5 min. Next, heat was again applied at 800 W for 3 min and then left again for 5 min. Finally, heat was applied at 200 W for 1 min, before the slices were left to cool to room temperature. The sections were then blocked for 1 h at room temperature with 3% hydrogen peroxide methanol solution and BSA (MilliporeSigma), before incubation with the following primary antibodies: Anti-TGF-β (1:200; cat. no. A25313; ABclonal Biotech Co., Ltd.), anti-NLRP3 (1:200; cat. no. A5652; ABclonal Biotech Co., Ltd,) and anti-IL-1β (1:200; cat. no. ab315084; Abcam) overnight at 4˚C. Subsequently, the sections were washed with PBS and incubated with ready-to-use secondary antibodies from an immunohistochemistry kit (cat. no. PV-6000; Beijing Zhongshan Jinqiao Biotechnology Co., Ltd.) for 30 min at 37˚C. The sections were then stained with DAB Substrate Kit (Beijing Zhongshan Jinqiao Biotechnology Co. LTD., Beijing, China, cat. no. ZLI-9019) for 20 min at room temperature and with hematoxylin (Sangon Biotech, Shanghai, China) for 10 sec at room temperature. The slides were observed and scanned with an orthogonal fluorescence microscope (ZEISS Axio Vert. A1).

Nuclear plasma separation experiment. FLSs cells were collected and resuspended with 100 μl buffer A [10 mM HEPES (pH 7.9), 10 mM KCl, 0.1 mM EDTA and 0.12% NP-40] and incubated for 15 min at 4˚C before centrifugation at 1,000 x g for 5 min at 4˚C to remove the supernatant and storage at -80˚C (cytoplasmic). The precipitate was washed three times with buffer A and washed with 150 μl buffer B [20 mM HEPES (pH 7.9), 0.4 mM NaCl, 1 mM EDTA, 1 mM EGTA and 0.5% NP-40]. After centrifugation at 1,000 x g for 5 min at 4˚C, the supernatant was collected and stored at -80˚C (cytoplasmic). Samples were subsequently subjected to western blotting. Histone was used as a control for nuclear proteins and GAPDH as a control for plasma proteins.

Western blotting. The FLSs or synovial tissues from rats in the Control, KOA and KOA + dicoumarol groups were lysed with RIPA Solution (Thermo Fisher Scientific, Inc.) and western blotting was performed as previously described (34). The BCA assay was used for protein quantification and the mass of proteins loaded per lane was 20 μg. Subsequently, protein samples were separated by SDS-PAGE on 15% gels and were transferred onto nitrocellulose membranes. The membranes were then blocked with non-fat milk at room temperature for 1 h and incubated at 4˚C for 24 h with primary antibodies. Subsequently, the membranes were incubated with secondary antibodies at room temperature for 1 h. Blot visualization was performed according to the manufacturer's instructions using the High-sig ECL Western Blot Substrate (cat. no. 180-5001) and Fully Automatic Chemiluminescence Image Analysis System (both from Tanon Science and Technology Co., Ltd.).

The following primary antibodies were used: Anti-TGF-β (1:1,000; cat. no. A2124), anti-TIMP1 (1:1,000; cat. no. A4959), anti-COL1A1 (1:1,000; cat. no. A1352), anti-IL-1β (1:1,000; cat. no. A16288), anti-IL-18 (1:1,000; cat. no. A1115), anti-NLRP3 (1:1,000; cat. no. A12694), anti-GSDMD (1:1,000; cat. no. A20728; both cleaved and total GSDMD), anti-ASC (1:1,000; cat. no. A16672), anti-NF-κB (1:1,000; cat. no. A22279), anti-Histone (1:100,000; cat. no. A2348), anti-GAPDH (1:100,000; cat. no. AC001) and anti-β-actin (1:100,000; cat. no. AC026). The following secondary antibodies were used: HRP Goat Anti-Rabbit IgG (H+L) (cat. no. AS014) and HRP Goat Anti-Mouse IgG (H+L) (cat. no. AS003). All antibodies were purchased from ABclonal Biotech Co., Ltd. The HRP Goat Anti-Rabbit IgG (H+L) was used to detect TGF-β, TIMP1, COL1A1, IL-1β, IL-18, NLRP3, GSDMD, ASC, NF-κB, Histone and GAPDH. The HRP Goat Anti-Mouse IgG (H+L) was used to detect β-actin.

Reverse transcription-quantitative PCR (RT-qPCR). Total RNA was isolated from FLSs with TRIzol® (Invitrogen; Thermo Fisher Scientific, Inc.). RNA (1 μg) was used to generate cDNA using the Reverse Transcriptase kit (Vazyme Biotech Co., Ltd.) according to the manufacturer's protocol. Subsequently, SYBR green-based qPCR assay (Vazyme Biotech Co., Ltd.) was used to detect the transcriptional levels

Table I. Primer sequences for reverse transcription-quantitative PCR assay.

Gene	Forward	Reverse
Gapdh	5'-TTCACCACCATGGAGAAGGC-3'	5'-CTCGTGGTTCACACCCATCA-3'
Il1b	5'-ACAGCAGCATCTCGACAAGAGC-3'	5'-CCACGGGCAAGACATAGGTAGC-3'
Il18	5'-TCTGTAGCTCCATGCTTTCCG-3'	5'-GATCCTGGAGGTTGCAGAAGA-3'
Tgfb	5'-GACTCTCCACCTGCAAGACC-3'	5'-GGACTGGCGAGCCTTAGTTT-3'
Timp	5'-CAGCTTTCTGCAACTCGGAC-3'	5'-CAGCGTCGAATCCTTTGAGC-3'
Nlrp3	5'-GAGCTGGACCTCAGTGACAATGC-3'	5'-ACCAATGCGAGATCCTGACAACAC-3'
Col1a	5'-GATCCTGGAGGTTGCAGAAGA-3'	5'-AAGTTCCGGTGTGACTCGTG-3'

Il, interleukin; *Nlrp3*, NOD-like receptor protein 3.

of *Il1b*, *Il18*, *Tgfb*, *Timp*, *Nlrp3*, *Col1a* and *Gapdh*. Briefly, 2X AceQ qPCR SYBR Green Master Mix, primers, cDNA and ddH_2O were combined in a sterile, nuclease-free tube at a final reaction volume of 20 μl. qPCR was performed using the Applied Biosystems 7500 Fast RT-PCR (Becton, Dickinson and Company) under the following conditions: Initial denaturation at 95˚C for 5 min; followed by 40 cycles at 95˚C for 10 sec and 60˚C for 30 sec. The mRNA expression levels of the individual genes were normalized to *Gapdh* and calculated using the $2^{-\Delta\Delta Cq}$ data analysis method (35). Samples were normalized relative to the expression of the endogenous control gene *Gapdh*. Primer sequences are shown in Table I.

Cell viability assay. Cell Counting Kit (CCK)-8 was used to detect the effects of dicoumarol on the viability of FLSs. Cells were cultured in 96-well plates. When the cell density reached 85-90%, they were treated with different concentrations of dicoumarol (0, 0.4, 0.78, 1.56, 3.13, 6.25, 12.5, 25, 50 and 100 μM) for 24 h at 37˚C. Then, 10 μl CCK-8 solution (Shanghai Yeasen Biotechnology Co., Ltd.) was added to each well and the cells were placed in an incubator for 2 h at 37˚C. The optical density of the wells was detected at 450 nm using a microplate spectrophotometer (BioTek Instruments, Inc.). The IC_{50} values were calculated by non-linear regression analysis with the sigmoidal dose response with variable slope equation (GraphPad Prism 8.0; Dotmatics): Y=1/[1 + 10^(logIC_{50}- X) (Hillslope)].

Flow cytometry. Apoptosis was detected using the Annexin V-FITC/PI Apoptosis Detection Kit (Vazyme Biotech Co., Ltd.). After treatment, FLSs were double stained with 1% Annexin V dye and PI dye for 20 min at room temperature. Apoptotic cells were subsequently analyzed using a BD FACS ARIA II SORP (BD Biosciences). The ModFit LT 5.0 (Verity Software House, Inc.) was used to measure the total apoptosis rate in the present study.

Statistical analysis. The statistical analysis was performed using GraphPad Prism 8. Data are presented as the mean ± standard deviation from at least three independent experiments. Statistical normality and variance homogeneity was assessed, and significance was determined by unpaired Student's t-test or one-way ANOVA with Tukey's post hoc test. $P<0.05$ was considered to indicate a statistically significant difference.

Results

Dicoumarol protects rat synoviocytes from fibrosis and inflammation. FLSs have been identified as key drivers of inflammatory joint destruction in OA (36). Therefore, primary FLSs were separated from rat synovial tissues and validated by microscopic observation of cell morphology. To test the inhibitory effect of dicoumarol (the structure of which is shown in Fig. 1A) on cell viability, a CCK-8 assay was performed. Dicoumarol inhibited the viability of FLSs in a concentration-dependent manner, and the IC_{50} of dicoumarol was ~95.21 μM (Fig. 1B). To exclude the influence of dicoumarol on viability, a concentration of 30 μM was used in the subsequent experiments. To simulate inflammation during KOA progression, the combination of LPS and ATP was used to trigger the activation of inflammasomes and apoptosis. The results showed that the combination of LPS and ATP could significantly induce the apoptosis of FLSs; the apoptosis rate was increased to 35.77%. By contrast, dicoumarol could alleviate apoptosis and the apoptosis rate was decreased to 8.25% (Fig. 1C). In KOA, inflammation can increase the deposition of extracellular matrix and lead to synovial fibrosis. Therefore, western blot analysis was performed to evaluate the expression levels of fibrosis-related biomarkers. Western blot analysis showed that the expression levels of TGF-β (relative expression, 1.51), TIMP1 (2.20) and COL1A1 (1.49) were significantly elevated in the LPS + ATP-treated group compared with the expression of TGF-β (0.68), TIMP1 (0.84) and COL1A1 (0.72) in the control group (Fig. 1D). Notably, the expression levels of these proteins could be suppressed by dicoumarol, and the protein expression levels of TGF-β, TIMP1 and COL1A1 decreased to 0.61, 1.07 and 0.70, respectively. The NLRP3 inflammasomes are key regulators that promote the secretion of proinflammatory cytokines, such as IL-1β and IL-18 (37,38). Western blot analysis showed that the expression levels of IL-β (0.98) and IL-18 (1.43) were significantly elevated in the LPS + ATP-treated group compared with the expression of IL-β (0.50) and IL-18 (0.66) in the control group, and the expression could be decreased to 0.59 and 0.70 by dicoumarin, respectively (Fig. 1E). Subsequently, the mRNA expression levels of these fibrotic and inflammatory markers were detected by RT-qPCR. The combination of LPS and ATP could increase mRNA expression levels of *Tgfb* (1.28), *Timp* (1.57), *Col1a1* (3.11), *Il1b* (2.38) and *Il18* (2.11), while

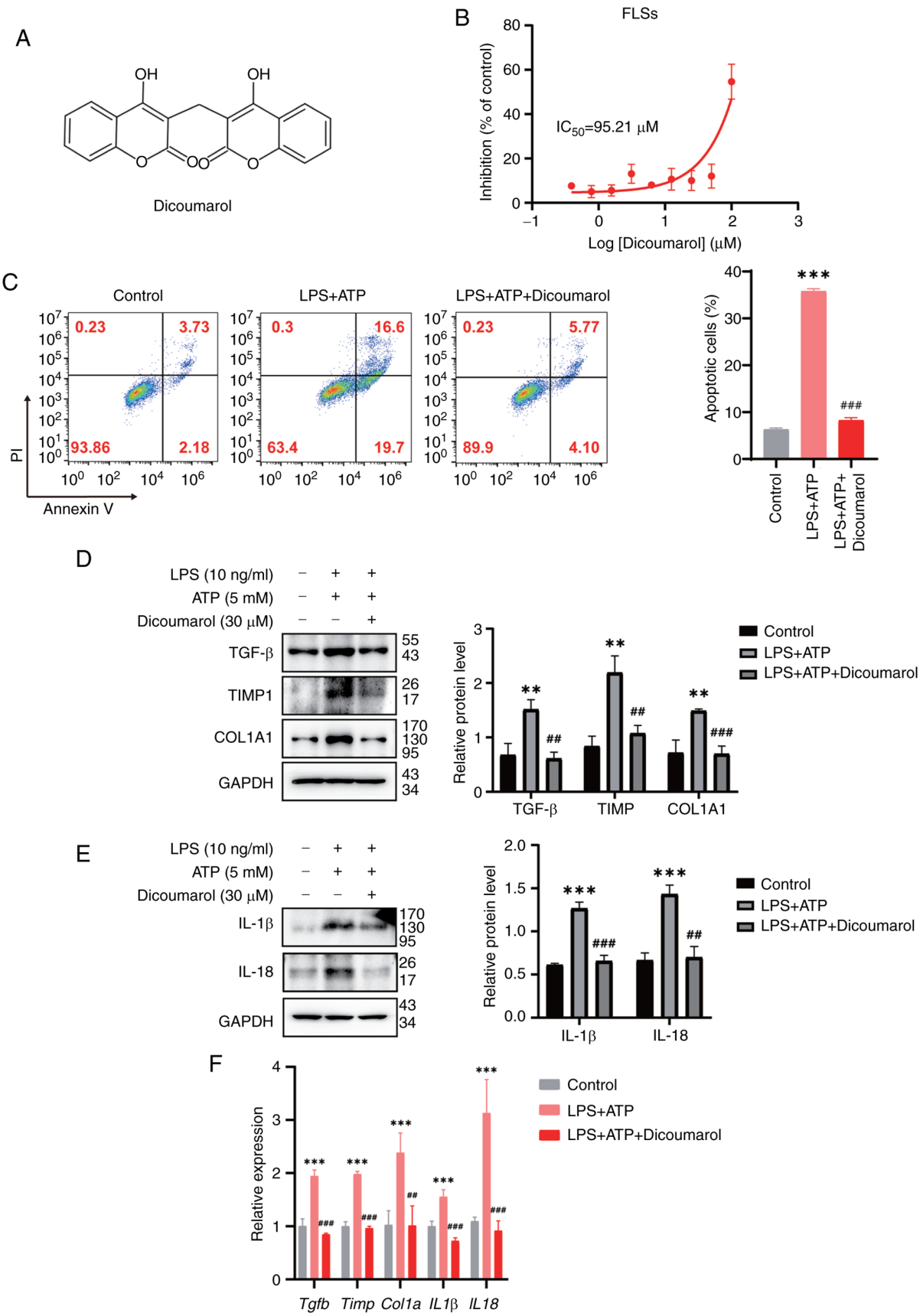

Figure 1. Dicoumarol protects rat synoviocytes from fibrosis and inflammation. (A) Chemical structure of dicoumarol. (B) FLSs were treated with the indicated concentrations of dicoumarol for 72 h. Cell viability was detected by Cell Counting Kit-8 assay. This part of the experiment was repeated three times. (C-F) FLSs were initially stimulated with LPS (10 ng/ml) for 12 h, followed by a 3-h incubation with ATP (5 mM), and were subsequently treated with dicoumarol (30 μM) for an additional 12 h. This part of the experiment was repeated three times. (C) Cells were stained with Annexin-V FITC/PI and flow cytometry was carried out to assess apoptosis. Western blot analysis of (D) fibrosis-related proteins and (E) inflammation-related proteins. (F) Quantification of mRNA expression levels of *Tgfb*, *Timp*, *Col1α*, *Il1b* and *Il18*. **P<0.01, ***P<0.001 vs. control group; $^{\#\#}$P<0.01, $^{\#\#\#}$P<0.001 vs. LPS + ATP group. FLS, fibroblast-like synoviocyte; IL, interleukin; LPS, lipopolysaccharide.

they were all reduced after dicoumarol treatment (Fig. 1F). The mRNA expression levels of *Tgfb*, *Timp*, *Col1a1*, *Il1b* and *Il18* in dicoumarol-treated FLSs were 1.02, 0.77, 1.62, 0.77 and 1.02, respectively. These results indicated that dicoumarol could inhibit fibrosis and inflammation in KOA.

Dicoumarol specifically binds to NLRP3 to inhibit its expression. The present study aimed to uncover the mechanism underlying the effects of dicoumarol on KOA. Since dicoumarol was demonstrated to inhibit the secretion of proinflammatory cytokines, it was hypothesized that dicoumarol could directly bind to the NLRP3 inflammasome and decrease its activation to inhibit apoptosis. Firstly, to determine the binding ability between dicoumarol and NLRP3 in FLSs, a CETSA was performed. Western blot analysis showed that the protein stability of NLRP3 in FLSs decreased with increasing temperature (Fig. 2A). At 57.2˚C, the protein expression levels of NLRP3 in the dicoumarol-treated group (0.803) were markedly higher than those (0.541) in the control group, indicating that the interaction between dicoumarol and NLRP3 enhances the thermostability of NLRP3. Subsequently, FLSs were treated with various concentrations of dicoumarol at 52˚C. The results revealed that the protein expression levels of NLRP3 increased from 0.012 to 0.869 as the concentration of dicoumarol increased (Fig. 2B). The present study also revealed that the combination of LPS and ATP could increase the expression levels of NLRP3 (1.51) and cleaved-GSDMD (1.41) compared with the expression of NLRP3 (1.06) and cleaved-GSDMD (1.10) in the control group, whereas the expression levels of ASC (adaptor protein of NLRP3) were not changed (Fig. 2C). Notably, dicoumarol could reduce the elevated expression levels of NLRP3 (0.98) and cleaved-GSDMD (0.94). To investigate whether the effect of dicoumarol was at the transcriptional level, the mRNA expression levels of *Nlrp3* were assessed. However, various concentrations of dicoumarol did not inhibit the mRNA expression levels of *Nlrp3*; the relative expression levels of *Nlrp3* were 1.00, 0.96 and 0.91 in response to 12.5, 25 and 50 μM dicoumarol, respectively (Fig. 2D). In summary, dicoumarol could interact with NLRP3 to enhance its thermostability, inhibit its expression and ultimately block cell apoptosis.

Dicoumarol promotes NLRP3 degradation through the ubiquitin-proteasome system. NF-κB serves an important role in the response to inflammatory stress and the activation of NLRP3 (13,39). Since coumarin compounds often inhibit NF-κB signaling, the present study aimed to determine whether dicoumarol could inhibit NLRP3 expression by blocking the NF-κB pathway. The results revealed that dicoumarol could not suppress the nuclear translocation of NF-κB p65, which was induced by combination of LPS and ATP (Fig. 3A). Subsequently, the present study aimed to determine whether dicoumarol inhibited NLRP3 expression by promoting its degradation. Thus, FLSs were treated with CHX, a protein synthesis inhibitor, at the specified time points with DMSO or dicoumarol. In the control group, the protein expression levels of NLRP3 started to markedly decrease at 12 h, whereas in the dicoumarol-treated group, the protein expression levels of NLRP3 obviously decreased at 2 h (Fig. 3B). Dicoumarol could reduce the protein half-life of NLRP3 from 26.1 to 4.3 h, suggesting that dicoumarol promoted the degradation of NLRP3. To reveal the detailed ways in which dicoumarol promoted NLRP3 degradation, FLSs were treated with MG132, a proteasome inhibitor, to block the proteasomal degradation pathway. The western blot analysis showed that the expression levels of NLRP3 (1.90) in the LPS + ATP-treated group were increased compared with those (1.16) in the control group, whereas dicoumarol decreased the expression to 0. 98 (Fig. 3C). When MG132 was added to block the proteasomal degradation pathway, dicoumarol could not further decrease the NLRP3 expression that was elevated by LPS and ATP. Subsequently, FLSs were treated with NH_4Cl, a lysosomal inhibitor, to block the lysosomal degradation pathway. Western blotting showed that the expression levels of NLRP3 (1.96) in the LPS + ATP-treated group were increased compared with those (1.36) in the control group, and dicoumarol decreased the expression to 1.06 (Fig. 3D). When NH_4Cl was added to block the proteasomal degradation pathway, there was no impact on the aforementioned results. NLRP3 expression (1.77) in the LPS + ATP-treated group was still increased compared with that (1.16) in the control group, and dicoumarol decreased the expression to 1.04. Therefore, the degradation of NLRP3 was obstructed by MG132, but not NH_4Cl.

Dicoumarol relieves synovitis induced by MIA. To study the *in vivo* effect of dicoumarol on KOA, the rat model of MIA-induced KOA was used. On day 28, the knee joint diameter in the control group was 9.04 mm and the knee joint diameter in the model group was 11.03 mm, which was significantly larger than that in the control group (Fig. 4A). Dicoumarol significantly reduced the knee joint diameter (9.93 mm) compared with that in the KOA group (Fig. 4A). Moreover, the anatomical characteristics and pathological sections of synovial tissue were observed to assess synovial fibrosis in rats. As determined by H&E and Sirius Red staining, intima formation, resident cell proliferation and inflammatory infiltration were reduced in dicoumarol-treated rats (Fig. 4B). Subsequently, synovial tissues were collected and prepared for western blotting and immunohistochemistry. Western blot analysis showed that the expression levels of IL-β (1.57) and IL-18 (1.22) were elevated in the model group compared with the expression of IL-β (0.45) and IL-18 (0.53) in the vehicle group, and the expression could be decreased to 0.49 and 0.44 by dicoumarol, respectively (Fig. 4C). In addition, western blot analysis showed that the expression levels of NLRP3 (2.62), TIMP1 (2.19) and COL1A1 (1.26) were significantly elevated in the model group compared with the expression of NLRP3 (0.54), TIMP1 (0.84) and COL1A1 (0.34) in the vehicle group; however, their expression could be suppressed by dicoumarol, and the protein expression levels of NLRP3, TIMP1 and COL1A1 decreased to 0.59, 0.92 and 0.31, respectively (Fig. 4D). Furthermore, the protein expression levels of NLRP3, TGF-β and IL-1β in the synovium of rats were measured by immunohistochemistry (Fig. 4E). Similarly, dicoumarol reduced the expression levels of NLRP3 in the synovium of rats compared with those in the KOA group, which resulted in reduced protein levels of the fibrosis-related biomarker TGF-β and the inflammation-related biomarker IL-1β.

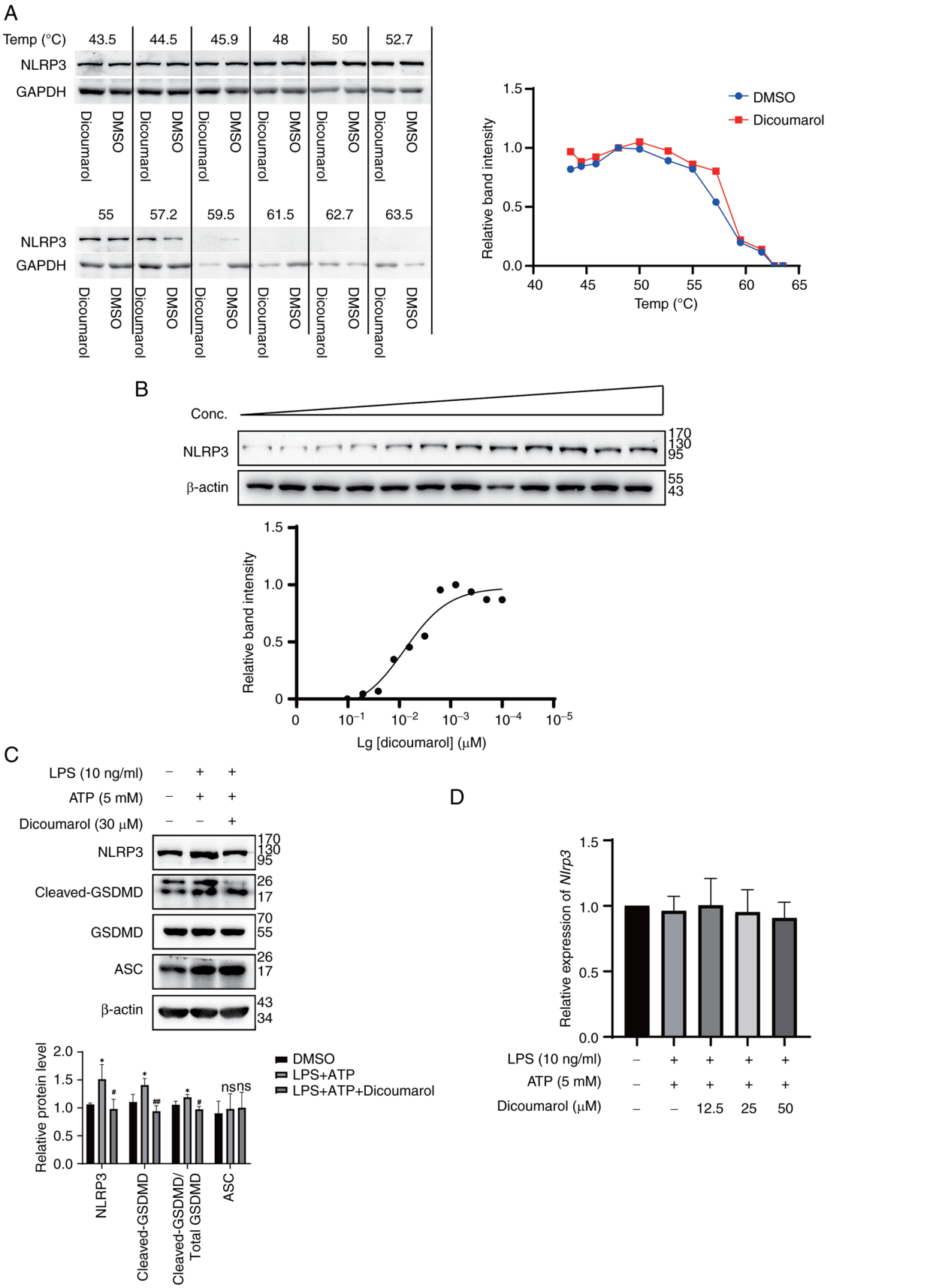

Figure 2. Dicoumarol binds to NLRP3 to inhibit its expression. (A) FLSs were treated with dicoumarol (30 μM) for 1 h. After shocking at the indicated temperatures and freeze-thaw cycles, the thermostability of NLRP3 was determined by western blot analysis. (B) FLSs were treated with different concentrations of dicoumarol for 1 h. NLRP3 expression was detected by western blot analysis. (C and D) FLSs were initially stimulated with LPS (10 ng/ml) for 12 h, followed by a 3-h incubation with ATP (5 mM), and were subsequently treated with dicoumarol (30 μM) for an additional 12 h. (C) Western blot analysis of NLRP3, GSDMD, cleaved-GSDMD and ASC. (D) Quantification of mRNA expression levels of *Nlrp3*. *P<0.05 vs. control group; $^{\#}$P<0.05, $^{\#\#}$P<0.01 vs. LPS + ATP group. ASC, apoptosis-related speckle-like protein; FLS, fibroblast-like synoviocyte; GSDMD, gasdermin-D; LPS, lipopolysaccharide; NLRP3, NOD-like receptor protein 3; ns, not significant.

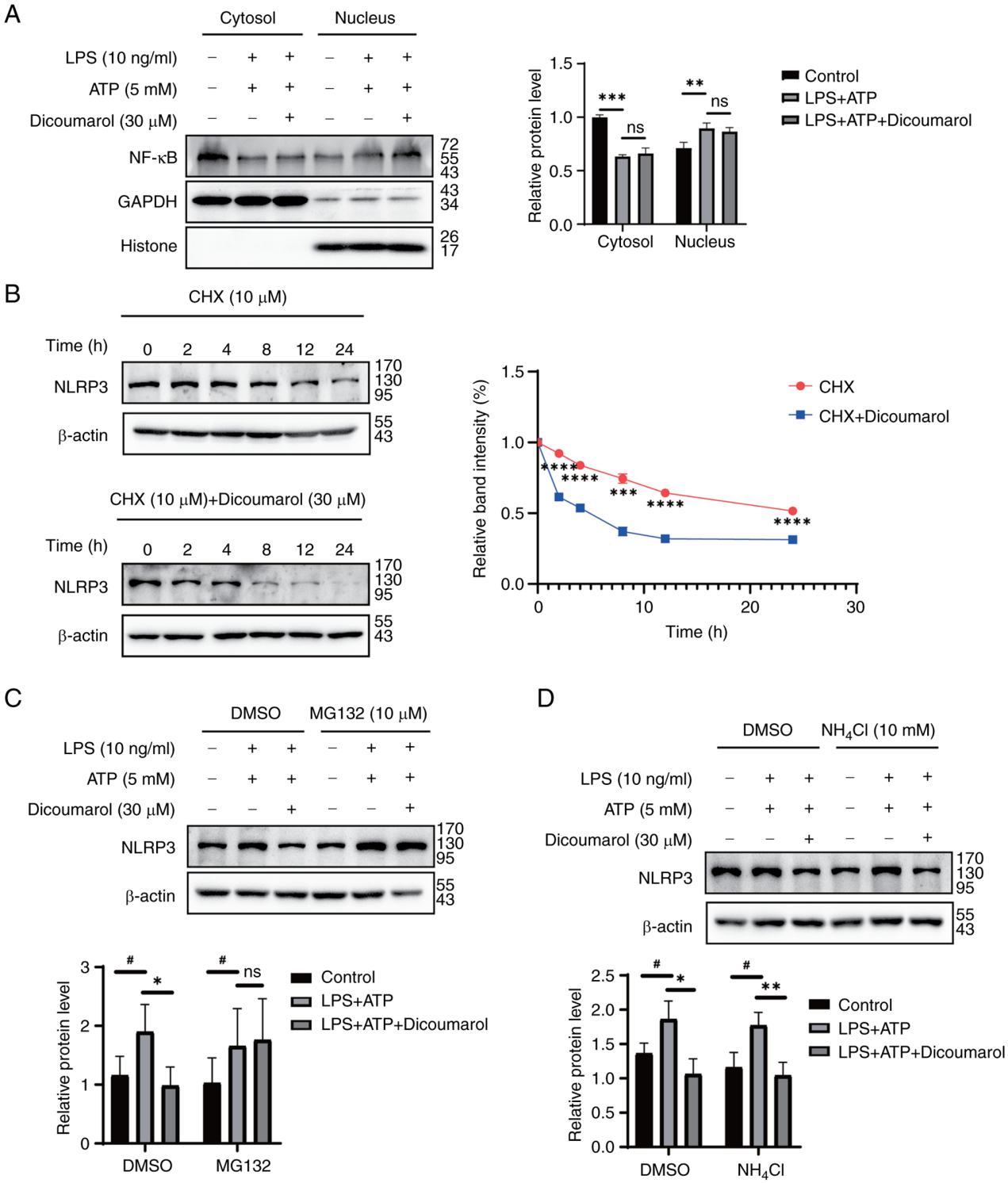

Figure 3. Dicoumarol promotes NLRP3 degradation through the ubiquitin-proteasome system. (A) FLSs were initially stimulated with LPS (10 ng/ml) for 12 h, followed by a 3-h incubation with ATP (5 mM), and were subsequently treated with dicoumarol (30 μM) for an additional 12 h. Western blot analysis of the expression of NF-κB in the cytoplasmic and nuclear extracts. (B) FLSs were pretreated with dicoumarol (30 μM) or DMSO for 12 h, followed by the addition of CHX (10 μg/ml) for various durations (0, 2, 4, 8, 12 and 24 h), after which the cells were harvested and western blot analysis of NLRP3 was performed. ***P<0.001, ****P<0.0001 vs. CHX + dicoumarol group. FLSs were stimulated with LPS (10 ng/ml) for 12 h, followed by a 3-h stimulation with ATP (5 mM). After a 12-h treatment with dicoumarol (30 μM), the cells were treated with (C) MG132 (10 μM) or (D) NH_4Cl (10 mM) for 8 h, the cells were collected and western blot analysis of NLRP3 was performed. *P<0.05, **P<0.01 (LPS + ATP group vs. LPS + ATP + dicoumarol group); $^{\#}$P<0.05 (control vs. LPS + ATP group). CHX, cycloheximide; FLS, fibroblast-like synoviocyte; LPS, lipopolysaccharide; NLRP3, NOD-like receptor protein 3; ns, not significant.

Discussion

NLRP3 is a polyprotein oligomer composed of caspase-1, ASC and NLRP3. After activation, NLRP3 interacts with ASC to bridge NLRP3 to procaspase-1, which activates caspase-1 (40). Activated caspase-1 cleaves the original forms of IL-1β and IL-18 into mature and active forms (41). Notably, IL-1β and IL-18 are key inflammatory factors in the pathological process

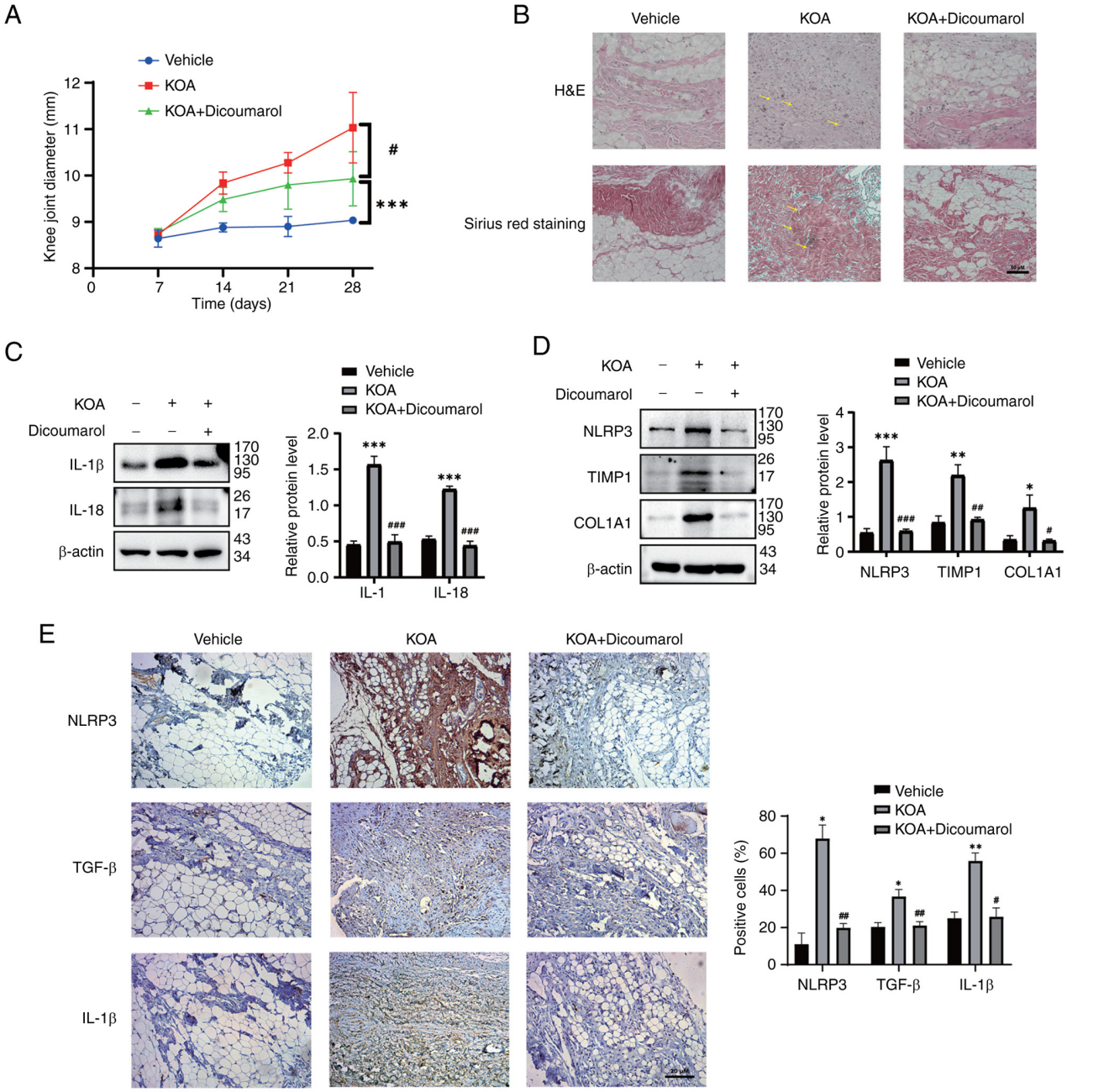

Figure 4. Dicoumarol relieves synovitis induced by MIA. (A-E) Rats were divided into the vehicle group (n=7), KOA group (n=7) and KOA + dicoumarol group (n=7). After the rat KOA model was established via the injection of a suspension of MIA, the rats were treated with normal saline or 10 mg/kg dicoumarol every day. (A) Diameters of right knees were evaluated to assess the severity of synovial fibrosis. $^{\#}$P<0.05 vs. control group. ***P<0.01 compared with KOA group. (B) Anatomical changes of each group. Representative synovial tissues of each group stained with H&E or Sirius Red. Scale bar, 50 μm. The lesion area is indicated by yellow arrows. Expression levels of (C) IL-1β and IL-18, and (D) NLRP3, TIMP1 and COL1A1 of synovial tissues in each group were detected. (E) Immunohistochemical staining of NLRP3, TGF-β and IL-1β in synovial tissues of each group. Scale bar, 20 μm. *P<0.05, **P<0.01, ***P<0.001 vs. normal group; $^{\#}$P<0.05, $^{\#\#}$P<0.01, $^{\#\#\#}$P<0.001 vs. KOA group. H&E, hematoxylin and eosin; IL, interleukin; KOA, knee osteoarthritis; MIA, monosodium iodoacetate; NLRP3, NOD-like receptor protein 3.

of synovitis. The results of the present study demonstrated that dicoumarol could protect against inflammasome-induced cell death through decreasing NLRP3 expression, which consistently reduced the expression of IL-1β and IL-18. Therefore, treatments that reduce the secretion of these two inflammatory factors may be a reliable method to treat synovial inflammation and fibrosis to delay the progression of KOA.

KOA has become a common disorder in an increasingly aging society (42,43). Several pathogenic factors of KOA have been discovered; however, the pathogenesis is still unclear. The occurrence of KOA is related to age, obesity, inflammation, trauma and genetic factors (1,5). The main features of KOA include synovitis, cartilage destruction and osteophyte formation, which results in a serious burden to the daily life of patients (44-46). Patients with severe KOA may even be permanently disabled, negatively affecting the physical and mental health of these patients, which can produce a burden on the health system and social economy. In the present study, it was revealed that dicoumarol inhibited the progression of KOA through improving

inflammation and fibrosis. To the best of our knowledge, this effect has not been previously reported in the study of dicoumarol. Due to the key role of NLRP3 in inflammatory cascade amplification, inhibiting NLRP3 expression has become the focus of anti-inflammatory therapy. The NLRP3 inflammasome is closely related to the pathogenesis of KOA, and is involved in cartilage destruction and synovitis in KOA (30). Various herbal extracts have been shown to block activation of the NLRP3 inflammasome with fewer side effects (47). For example, coumarins have been reported to exert anti-inflammatory effects by inhibiting NLRP3 activation (26,48). However, fewer compounds could alleviate inflammation by inhibiting NLRP3. The present study found that dicoumarol directly interacted with NLRP3 in FLSs, which offers novel compounds for specific inhibitors of NLRP3. However, the affinity between dicoumarol and NLRP3 was not further tested; therefore, our future studies aim to advance the related research and optimize the structure of dicoumarol.

The present study demonstrated that dicoumarol inhibited the protein expression levels of NLRP3 and cleaved-GSDMD in FLSs, rather than mRNA expression, suggesting that dicoumarol suppressed NLRP3 expression at the post-transcriptional level. Hence, the protein degradation pathway of NLRP3 was examined. MG132, but not NH_4Cl, could block the degradation of NLRP3 induced by dicoumarol, which suggested that the ubiquitin-proteasome system was involved in the process of dicoumarol-decreased NLRP3 expression. The main pathological features of KOA include cartilage matrix synovitis and chondrocyte reduction (49). In *in vivo* experiments, it was revealed that dicoumarol reduced the knee joint diameter during the progression of KOA. Meanwhile, dicoumarol inhibited collagen deposition and inflammatory cell infiltration. Under pathological conditions, inflammatory cells can infiltrate the joint synovium, and then release a large number of inflammatory factors, chemokines and proteases, which can also be reduced by dicoumarol *in vivo*. Although the inhibitory effect of dicoumarol on OA is clearly defined in the present study, the potential toxicity and pharmacokinetic profile have not been studied, which are important factors for the application of dicoumarol in clinical treatments.

Collectively, the present study demonstrated that dicoumarol can alleviate the development of KOA *in vivo* and *in vitro*. Furthermore, it was confirmed that dicoumarol can interact with NLRP3 and degrade NLRP3 through the ubiquitin-proteasome pathway. However, the present study has some limitations. The mechanism by which dicoumarol inhibit fibrosis needs to be further investigated. In addition, the specific effects of dicoumarol in humans are still uncertain and need to be studied further. In future studies, we aim to use more animal models to further confirm the pharmacological effects of dicoumarol from the aspects of *in vitro* cell and animal experiments, and provide more reliable experimental data for its clinical application.

Acknowledgements

Not applicable.

Funding

This work was supported by a grant from the Youth Project of Wuxi Health Commission (grant no. Q201916).

Availability of data and materials

The data generated in the present study may be requested from the corresponding author.

Authors' contributions

WG designed experiments, and wrote and edited the manuscript. XZ and QW performed cell studies. JM and PJ performed animal studies. JC directed this project and analyzed the experimental data. WG and JC confirm the authenticity of all the raw data. All authors read and approved the final manuscript.

Ethics approval and consent to participate

All animal experiments were performed according to the National Institute of Health Animal Care and Use Guidelines. The protocol was approved by the committee for the Ethics of Animal Experiments, Wuxi Hospital of Traditional Chinese Medicine (approval no. SWJWQNXM2020033102).

Patient consent for publication

Not applicable.

Competing interests

The authors declare that they have no competing interests.

References

1. Lv Z, Yang YX, Li J, Fei Y, Guo H, Sun Z, Lu J, Xu X, Jiang Q, Ikegawa S and Shi D: Molecular classification of knee osteoarthritis. Front Cell Dev Biol 9: 725568, 2021.
2. Mintarjo JA, Poerwanto E and Tedyanto EH: Current non-surgical management of knee osteoarthritis. Cureus 15: e40966, 2023.
3. Onuora S: Osteoarthritis: OA chondrocytes made senescent by genomic DNA damage. Nat Rev Rheumatol 8: 502, 2012.
4. Dell'Isola A, Allan R, Smith SL, Marreiros SS and Steultjens M: Identification of clinical phenotypes in knee osteoarthritis: A systematic review of the literature. BMC Musculoskelet Disord 17: 425, 2016.
5. Du X, Liu ZY, Tao XX, Mei YL, Zhou DQ, Cheng K, Gao SL, Shi HY, Song C and Zhang XM: Research progress on the pathogenesis of knee osteoarthritis. Orthop Surg 15: 2213-2224, 2023.
6. Peloso P, Chen W, Lin HL, Gates D, Straus W and Moore R: (363) Pain improvement in osteoarthritis (OA) predicts improved functioning. J Pain 15 (Suppl): S66, 2014.
7. Li R, Sun J, Hu H, Zhang Q, Sun R, Zhou S, Zhang H and Fang J: Research trends of acupuncture therapy on knee osteoarthritis from 2010 to 2019: A bibliometric analysis. J Pain Res 13: 1901-1913, 2020.
8. Georgiev T and Angelov AK: Modifiable risk factors in knee osteoarthritis: Treatment implications. Rheumatol Int 39: 1145-1157, 2019.
9. Zhang J, Fan F, Liu A, Zhang C, Li Q, Zhang C, He F and Shang M: Icariin: A potential molecule for treatment of knee osteoarthritis. Front Pharmacol 13: 811808, 2022.
10. Yang X, Thudium CS, Bay-Jensen AC, Karsdal MA, van Santen J, Arden NK, Perry TA and Kluzek S: Association between markers of synovial inflammation, matrix turnover and symptoms in knee osteoarthritis: A cross-sectional study. Cells 10: 1826, 2021.

11. Li X, Mei W, Huang Z, Zhang L, Zhang L, Xu B, Shi X, Xiao Y, Ma Z, Liao T, *et al*: Casticin suppresses monoiodoacetic acid-induced knee osteoarthritis through inhibiting HIF-1α/NLRP3 inflammasome signaling. Int Immunopharmacol 86: 106745, 2020.
12. Tan Q, Cai Z, Li J, Li J, Xiang H, Li B and Cai G: Imaging study on acupuncture inhibiting inflammation and bone destruction in knee osteoarthritis induced by monosodium iodoacetate in rat model. J Pain Res 15: 93-103, 2022.
13. Jo EK, Kim JK, Shin DM and Sasakawa C: Molecular mechanisms regulating NLRP3 inflammasome activation. Cell Mol Immunol 13: 148-159, 2016.
14. Zhang L, Li X, Zhang H, Huang Z, Zhang N, Zhang L, Xing R and Wang P: Agnuside alleviates synovitis and fibrosis in knee osteoarthritis through the inhibition of HIF-1α and NLRP3 inflammasome. Mediators Inflamm 2021: 5534614, 2021.
15. Sharma BR and Kanneganti TD: NLRP3 inflammasome in cancer and metabolic diseases. Nat Immunol 22: 550-559, 2021.
16. Xu J and Núñez G: The NLRP3 inflammasome: Activation and regulation. Trends Biochem Sci 48: 331-344, 2023.
17. Zhou R, Yazdi AS, Menu P and Tschopp J: A role for mitochondria in NLRP3 inflammasome activation. Nature 469: 221-225, 2011.
18. Kaufmann FN, Costa AP, Ghisleni G, Diaz AP, Rodrigues ALS, Peluffo H and Kaster MP: NLRP3 inflammasome-driven pathways in depression: Clinical and preclinical findings. Brain Behav Immun 64: 367-383, 2017.
19. Afonina IS, Zhong Z, Karin M and Beyaert R: Limiting inflammation-the negative regulation of NF-κB and the NLRP3 inflammasome. Nat Immunol 18: 861-869, 2017.
20. Conway R and McCarthy GM: Calcium-containing crystals and osteoarthritis: An unhealthy alliance. Curr Rheumatol Rep 20: 13, 2018.
21. Kapoor M, Martel-Pelletier J, Lajeunesse D, Pelletier JP and Fahmi H: Role of proinflammatory cytokines in the pathophysiology of osteoarthritis. Nat Rev Rheumatol 7: 33-42, 2011.
22. Ding L, Liao T, Yang N, Wei Y, Xing R, Wu P, Li X, Mao J and Wang P: Chrysin ameliorates synovitis and fibrosis of osteoarthritic fibroblast-like synoviocytes in rats through PERK/TXNIP/NLRP3 signaling. Front Pharmacol 14: 1170243, 2023.
23. Zhao LR, Xing RL, Wang PM, Zhang NS, Yin SJ, Li XC and Zhang L: NLRP1 and NLRP3 inflammasomes mediate LPS/ATP-induced pyroptosis in knee osteoarthritis. Mol Med Rep 17: 5463-5469, 2018.
24. Ma Z, Huang Z, Zhang L, Li X, Xu B, Xiao Y, Shi X, Zhang H, Liao T and Wang P: Vanillic acid reduces pain-related behavior in knee osteoarthritis rats through the inhibition of NLRP3 inflammasome-related synovitis. Front Pharmacol 11: 599022, 2021.
25. Sun C, Zhao W, Wang X, Sun Y and Chen X: A pharmacological review of dicoumarol: An old natural anticoagulant agent. Pharmacol Res 160: 105193, 2020.
26. Chkhikvishvili I, Mamniashvili T, Gogia N, Enukidze M, Machavariani M and Sanikidze T: Antioxidant, anti-inflammatory activity of georgian leguminous crops cultures. Georgian Med News: 147-153, 2017.
27. Timson DJ: Dicoumarol: A drug which hits at least two very different targets in vitamin K metabolism. Curr Drug Targets 18: 500-510, 2017.
28. PERONNET: Anticoagulants, heparin and dicoumarol. Fr Med 11: 3-8, 1948 (In French).
29. Council NJP: Guide for the Care and Use of Laboratory Animals. 8th edition. National Academies Press, Washington, DC, pp963-965, 2010.
30. Liao T, Ding L, Wu P, Zhang L, Li X, Xu B, Zhang H, Ma Z, Xiao Y and Wang P: Chrysin attenuates the NLRP3 inflammasome cascade to reduce synovitis and pain in KOA rats. Drug Des Devel Ther 14: 3015-3027, 2020.
31. Cheng ST, Hu JL, Ren JH, Yu HB, Zhong S, Wai Wong VK, Kwan Law BY, Chen WX, Xu HM, Zhang ZZ, *et al*: Dicoumarol, an NQO1 inhibitor, blocks cccDNA transcription by promoting degradation of HBx. J Hepatol 74: 522-534, 2021.
32. Shi J, Zhao W, Ying H, Zhang Y, Du J, Chen S, Li J and Shen B: Estradiol inhibits NLRP3 inflammasome in fibroblast-like synoviocytes activated by lipopolysaccharide and adenosine triphosphate. Int J Rheum Dis 21: 2002-2010, 2018.
33. Zhang L, Xu J, Zhou S, Yao F, Zhang R, You W, Dai J, Yu K, Zhang Y, Baheti T, *et al*: Endothelial DGKG promotes tumor angiogenesis and immune evasion in hepatocellular carcinoma. J Hepatol 80: 82-98, 2024.
34. Nàger M, Sallán MC, Visa A, Pushparaj C, Santacana M, Macià A, Yeramian A, Cantí C and Herreros J: Inhibition of WNT-CTNNB1 signaling upregulates SQSTM1 and sensitizes glioblastoma cells to autophagy blockers. Autophagy 14: 619-636, 2018.
35. Livak KJ and Schmittgen TD: Analysis of relative gene expression data using real-time quantitative PCR and the 2(-Delta Delta C(T)) method. Methods 25: 402-408, 2001.
36. Bhattaram P and Chandrasekharan U: The joint synovium: A critical determinant of articular cartilage fate in inflammatory joint diseases. Semin Cell Dev Biol 62: 86-93, 2017.
37. Toldo S, Mezzaroma E, Buckley LF, Potere N, Di Nisio M, Biondi-Zoccai G, Van Tassell BW and Abbate A: Targeting the NLRP3 inflammasome in cardiovascular diseases. Pharmacol Ther 236: 108053, 2022.
38. Shao BZ, Xu ZQ, Han BZ, Su DF and Liu C: NLRP3 inflammasome and its inhibitors: A review. Front Pharmacol 6: 262, 2015.
39. He Y, Hara H and Núñez G: Mechanism and regulation of NLRP3 inflammasome activation. Trends Biochem Sci 41: 1012-1021, 2016.
40. Lu A, Magupalli VG, Ruan J, Yin Q, Atianand MK, Vos MR, Schröder GF, Fitzgerald KA, Wu H and Egelman EH: Unified polymerization mechanism for the assembly of ASC-dependent inflammasomes. Cell 156: 1193-1206, 2014.
41. Elliott EI and Sutterwala FS: Initiation and perpetuation of NLRP3 inflammasome activation and assembly. Immunol Rev 265: 35-52, 2015.
42. Shimizu H, Shimoura K, Iijima H, Suzuki Y and Aoyama T: Functional manifestations of early knee osteoarthritis: A systematic review and meta-analysis. Clin Rheumatol 41: 2625-2634, 2022.
43. Rannou F and Poiraudeau S: Non-pharmacological approaches for the treatment of osteoarthritis. Best Pract Res Clin Rheumatol 24: 93-106, 2010.
44. Geng R, Li J, Yu C, Zhang C, Chen F, Chen J, Ni H, Wang J, Kang K, Wei Z, *et al*: Knee osteoarthritis: Current status and research progress in treatment (Review). Exp Ther Med 26: 481, 2023.
45. Okada K, Yamaguchi S, Sato Y, Enomoto T, Ogawa Y, Ohtori S, Tahara M and Sasho T: Comparison of meniscal extrusion and osteophyte formation at the intercondylar notch as a predictive biomarker for incidence of knee osteoarthritis-data from the osteoarthritis initiative. J Orthop Sci 24: 121-127, 2019.
46. Whittaker JL, Runhaar J, Bierma-Zeinstra S and Roos EM: A lifespan approach to osteoarthritis prevention. Osteoarthritis Cartilage 29: 1638-1653, 2021.
47. Wang M, Liu L, Zhang CS, Liao Z, Jing X, Fishers M, Zhao L, Xu X and Li B: Mechanism of traditional Chinese medicine in treating knee osteoarthritis. J Pain Res 13: 1421-1429, 2020.
48. Place DE and Kanneganti TD: Recent advances in inflammasome biology. Curr Opin Immunol 50: 32-38, 2018.
49. Samadfam R, Chouinard L, Norton K and Smith S: Pain assessment in monosodium iodoacetate (MIA)-induced osteoarthritis (OA) model. J Pharmacol Toxicol Methods 68: e39, 2013.